Detecting Stealth Dark Matter Directly through Electromagnetic Polarizability

T. Appelquist,[1] E. Berkowitz,[2] R. C. Brower,[3] M. I. Buchoff,[4] G. T. Fleming,[1] X.-Y. Jin,[5] J. Kiskis,[6]
G. D. Kribs,[7] E. T. Neil,[8,9] J. C. Osborn,[5] C. Rebbi,[3] E. Rinaldi,[2] D. Schaich,[10] C. Schroeder,[2] S. Syritsyn,[9]
P. Vranas,[2] E. Weinberg,[3] and O. Witzel[11,*]

(Lattice Strong Dynamics (LSD) Collaboration)

[1]*Department of Physics, Sloane Laboratory, Yale University, New Haven, Connecticut 06520, USA*
[2]*Lawrence Livermore National Laboratory, Livermore, California 94550, USA*
[3]*Department of Physics, Boston University, Boston, Massachusetts 02215, USA*
[4]*Institute for Nuclear Theory, Box 351550, Seattle, Washington 98195-1550, USA*
[5]*Argonne Leadership Computing Facility, Argonne, Illinois 60439, USA*
[6]*Department of Physics, University of California, Davis, California 95616, USA*
[7]*Department of Physics, University of Oregon, Eugene, Oregon 97403, USA*
[8]*Department of Physics, University of Colorado, Boulder, Colorado 80309, USA*
[9]*RIKEN-BNL Research Center, Brookhaven National Laboratory, Upton, New York 11973, USA*
[10]*Department of Physics, Syracuse University, Syracuse, New York 13244, USA*
[11]*Center for Computational Science, Boston University, Boston, Massachusetts 02215, USA*
(Received 30 May 2015; published 23 October 2015)

We calculate the spin-independent scattering cross section for direct detection that results from the electromagnetic polarizability of a composite scalar "stealth baryon" dark matter candidate, arising from a dark SU(4) confining gauge theory—"stealth dark matter." In the nonrelativistic limit, electromagnetic polarizability proceeds through a dimension-7 interaction leading to a very small scattering cross section for dark matter with weak-scale masses. This represents a lower bound on the scattering cross section for composite dark matter theories with electromagnetically charged constituents. We carry out lattice calculations of the polarizability for the lightest "baryon" states in SU(3) and SU(4) gauge theories using the background field method on quenched configurations. We find the polarizabilities of SU(3) and SU(4) to be comparable (within about 50%) normalized to the stealth baryon mass, which is suggestive for extensions to larger SU(N) groups. The resulting scattering cross sections with a xenon target are shown to be potentially detectable in the dark matter mass range of about 200–700 GeV, where the lower bound is from the existing LUX constraint while the upper bound is the coherent neutrino background. Significant uncertainties in the cross section remain due to the more complicated interaction of the polarizablity operator with nuclear structure; however, the steep dependence on the dark matter mass, $1/m_B^6$, suggests the observable dark matter mass range is not appreciably modified. We briefly highlight collider searches for the mesons in the theory as well as the indirect astrophysical effects that may also provide excellent probes of stealth dark matter.

Introduction.—Despite remarkable advances in direct detection experiments [1–4], a conclusive signal of nuclear interactions with dark matter (DM) remains elusive. These experiments, which are sensitive to nucleus-DM cross sections at or below 10^{-45} cm^2 per nucleon, have already excluded large classes of interactions and models, and are now actively probing Higgs boson exchange [3,4].

Composite DM, which arises as a neutral bound state of a strongly coupled gauge force (for early work, see Refs. [5–9]), has sparked multiple recent lattice calculations [10–17]. If its constituents are electromagnetically charged, the DM will interact with standard model (SM) nuclei via photon exchange, with the cross section suppressed by a momentum-dependent electromagnetic form factor. Expanding at small momentum transfer, one can obtain a series of effective operators describing the interaction: the dimension-5 magnetic moment, dimension-6 charge radius, and dimension-7 polarizability are the leading operators [18–20]. Symmetry considerations can give models in which the first two operators are identically zero [21,22]. Scattering due to electromagnetic polarizability remains, giving a lower bound on the direct detection cross section for a composite DM particle with charged constituents.

We will focus here on a particular composite DM model, "stealth dark matter" [23], in which the DM is a scalar "stealth baryon" composed of dark fermions that transform under an SU(N_D) theory with N_D even. (We note that our

results do not apply to mesonic bound states, which are used for several other models of composite dark matter in which the DM candidate is a pseudo-Goldstone boson [10,21,22,24–27]. Lattice calculations of mesonic polarizabilities similar to those we describe here could be undertaken for those models.) In this model, electroweak symmetry breaking proceeds through the SM Higgs mechanism. The dominant modes of interaction with the SM are the polarizability operator and direct Higgs boson exchange. The latter was studied in some detail in Refs. [14,23], placing bounds on the allowed dark matter coupling to the Higgs boson. In this work we study the polarizability, which unlike the Higgs interaction has no adjustable parameters, but rather is completely determined by the strong dynamics once the gauge group and matter content are specified.

SU(4) baryons and polarizabilities.—A full construction of the stealth DM model is given in Ref. [23]; here we briefly summarize the relevant details. The dark sector consists of an unbroken SU(4) gauge theory, which contains bosonic baryonic bound states made up of four constituent fermions. The DM candidate itself is a scalar made up of two pairs of fermions which are degenerate in mass and carry equal but opposite electric charges of $\pm 1/2$. Hence, there is no magnetic moment or charge radius, leaving just the electromagnetic polarizability as the dominant interaction with photons.

Previous estimates of the polarizability of a composite scalar have led to direct-detection cross sections on the order of 10^{-48} cm^2 [20], approaching the interaction strength at which background neutrinos are expected to contaminate the DM recoil signal. However, the estimates were based on semiclassical calculations of a strongly coupled interaction, and so have uncontrolled uncertainties.

Additionally, due to how internal electric charges are correlated, the polarizability of bosonic 4-fermion baryons may differ appreciably from QCD-based estimates. In one limit where the internal constituents are uncorrelated, the polarizabilities are expected to be comparable. However, if alternate flavors tend to form pairs based on their Pauli statistics, the 4-fermion baryon polarizability would be derivative-suppressed compared to the 3-fermion baryon (i.e., two dipoles vs one dipole and one charge). In order to quantify this effect, we perform lattice calculations for both the SU(3) and SU(4) baryon polarizabilities.

Polarizability and direct detection.—The electric polarizability of the scalar baryonic composite DM field B with mass m_B can be written as an effective operator of the form

$$\mathcal{O}_F = C_F B^* B F^{\mu\alpha} F^\nu_\alpha v_\mu v_\nu \tag{1}$$

where $F_{\mu\nu}$ is the electromagnetic field strength tensor, $v_\mu = (1, 0, 0, 0)$ in the static limit, and C_F is the polarizability with mass dimension -3 in the nonrelativistic limit. Only the electric polarizability is considered since the magnetic

polarizability is expected to be suppressed [28]. This is a two-photon vertex, so that the scattering off of nuclei will involve a virtual photon loop. Because this operator is induced at a high scale (roughly the dark confinement scale $\Lambda_D \sim m_B$), it is expected to generate other interactions with SM particles when the appropriate effective field theory matching and running down to the nuclear scale are carried out [29–32]; in fact, an explicit treatment for the polarizability operator is given in Ref. [33]. Although the effects of the additional induced operators are not negligible in general, we find that they are small compared to the uncertainties (particularly from nuclear physics) and so we will omit them.

From the interaction shown above, the coherent DM-nucleus scattering cross section (per nucleon) is given by

$$\sigma_{\text{nucleon}}(Z, A) = \frac{\mu_{nB}^2}{\pi A^2} \langle |C_F f_F^A|^2 \rangle, \tag{2}$$

where m_n is the nucleon mass, $\mu_{nB} = m_n m_B/(m_n + m_B)$ is the reduced mass, (Z, A) are the atomic and mass numbers of the target nucleus, and the angular brackets represent the momentum-averaged form factors for heavy DM candidates in a given experiment [33].

The primary source of systematic uncertainty is on the nuclear physics side of the calculation—evaluating the nonperturbative nuclear matrix element, $f_F^A = \langle A| F^{\mu\nu} F_{\mu\nu} |A\rangle$. Various attempts to perturbatively estimate this matrix element have been performed with varying levels of complexity [33–35]. But, the matrix element also has nontrivial excited-state structures that likely require a fully nonperturbative treatment. This matrix element is similar to those needed for double-beta decay experiments, estimates for which have substantial variation [36,37]. Until a more accurate extraction of this matrix element is performed, we will use dimensional analysis arising from nonrelativistic loop momentum counting,

$$f_F^A \sim 3Z^2 \alpha \frac{M_F^A}{R}, \tag{3}$$

where $R = 1.2 A^{1/3}$ fm, as used in the double beta decay context, α is the fine-structure constant, and M_F^A is a dimensionless parameter. With the factor of 3 in Eq. (3), our expression approximately matches Refs. [33,34] for heavy nuclei when $M_F^A \simeq 1$. To allow for an order of magnitude uncertainty in the nuclear matrix element, we take $1/3 < M_F^A < 3$, although a detailed nuclear structure extraction would be needed for a more precise estimate.

Background field method.—In order to extract the electric polarizability from the lattice, the background field method is employed, as described in Refs. [38,39]. The essence of this method is to measure baryon two-point correlation functions in the presence of a uniform electric field $\mathcal{E}$. Working in Euclidean space, the background field

induces a quadratic Stark shift in the mass of the SU(4) ground-state baryon,

$$E_{B,4c} = m_B + 2C_F|\mathcal{E}|^2 + \mathcal{O}(\mathcal{E}^4), \tag{4}$$

where C_F is the desired polarizability, as defined in Eq. (1). (The electric polarizability of the neutron α_E is more commonly defined in terms of the induced dipole moment $\vec{d} = 4\pi\alpha_E\vec{\mathcal{E}}$, giving a quadratic Stark shift of $\Delta E_n = \frac{1}{2}\vec{d} \cdot \vec{\mathcal{E}} = 2\pi\alpha_E|\mathcal{E}|^2$. In our notation $\alpha_E = C_F/\pi$.)

Because of the scalar nature of the SU(4) baryon ground state, this relation is equivalent to what one would expect for mesons. For comparison we also study the fermionic SU(3) baryon, whose energy shift contains an additional contribution from the nonzero magnetic moment μ_B [39],

$$E_{B,3c} = m_B + \left(2C_F - \frac{\mu_B^2}{8m_B^3}\right)|\mathcal{E}|^2 + \mathcal{O}(\mathcal{E}^4). \tag{5}$$

For the SU(3) theory, we must therefore determine μ_B as well in order to extract C_F from the background field dependence.

The background field method is implemented following Refs. [38,39] where the uniform background field is included by multiplying the unitary gauge links by two phase terms, chosen so that the field is oriented in the $\hat{z}$ direction. Quantization of the uniform background field on a torus restricts the available field strengths to values

$$\mathcal{E}/a^2 = \frac{2\pi e n}{|q_{\text{low}}|N_t N_s}, \tag{6}$$

where a is the lattice spacing, e is the electromagnetic coupling, N_s and N_t are the number of spatial and temporal lattice sites, respectively, and q_{low} is the lowest common denominator of the charges [for SU(3), $q_{\text{low}} = 1/3$; for SU(4), $q_{\text{low}} = 1/2$].

For convenience we define a rescaled, dimensionless background field by $\tilde{\mathcal{E}} = (ea^2)^{-1}\mathcal{E}$. We will analyze our lattice results using Eqs. (4) and (5) with all quantities replaced with their rescaled, dimensionless counterparts, all of which will be denoted with a tilde:

$$m_B = \tilde{m}_B/a, \tag{7}$$

$$C_F = 4\pi\alpha a^3 \tilde{C}_F, \tag{8}$$

$$\mu_B = 4\pi\alpha\tilde{\mu}_B. \tag{9}$$

Lattice details and fitting.—The lattice calculations are done using the Chroma software package [40]. We use the plaquette gauge action with unimproved Wilson fermions. The gauge configurations are quenched $N_s^3 \times N_t = 32^3 \times 64$ lattices (20 000 heat-bath updates, 200 configurations

separated evenly). For SU(4) we choose $\beta = 11.028$ and for SU(3) $\beta = 6.0175$ following Ref. [41]. Fermionic propagators are calculated for two different masses at each N_D value ($\kappa = 0.1554, 0.15625$ for $N_D = 4$ and $\kappa = 0.1537, 0.1547$ for $N_D = 3$), chosen such that the ratio of the pseudoscalar to vector meson masses $m_{\text{PS}}/m_V = 0.77$ and 0.70 are matched [14,41].

Background field measurements are performed at six field values [$n = 0, ..., 5$, see Eq. (6)] for both $N_D = 4$ and $N_D = 3$, with correlation functions measured using 40 evenly separated sources in (x, y) along the $t = z = 0$ plane. Each zero and nonzero field value has 8000 measurements. All two-point correlation functions are fit over the range $t \in [4, 28]$ using fully correlated, multi-exponential fits including three excited states.

For $N_D = 4$, the two-point baryonic correlation function in background field $\tilde{\mathcal{E}}$ takes the form

$$C_B(t, \tilde{\mathcal{E}}) \sim Z(\tilde{\mathcal{E}}) \exp\left[-t\tilde{E}_B(\tilde{\mathcal{E}})\right] \tag{10}$$

at large t. Results for $\tilde{E}_B(\tilde{\mathcal{E}})$ are then fit to Eq. (4). We include higher-order contributions from the background field following Ref. [39],

$$\tilde{C}_F(\tilde{\mathcal{E}}) = \tilde{C}_F + \tilde{C}_F'|\tilde{\mathcal{E}}|^2. \tag{11}$$

The analysis for $N_D = 3$ is complicated by the contribution of the magnetic moment $\tilde{\mu}_B$ to the baryon self-energy. Following Ref. [39], we make use of the boost projections

$$\mathcal{P}_{\pm} = \frac{1}{2}(1 \pm i\gamma_3\gamma_4), \tag{12}$$

and the boosted correlators

$$\begin{aligned} C_B^{\pm}(t) &= \langle\bar{B}(\mathbf{x}, t)\mathcal{P}_{\pm}B(\mathbf{0}, 0)\rangle_{\mathcal{E}} \\ &= Z_{\pm}(\tilde{\mathcal{E}}) \exp\left[-t\tilde{E}_B(\tilde{\mathcal{E}})\right]. \end{aligned} \tag{13}$$

The boost-projected amplitudes $Z_{\pm}$ contain equal and opposite contributions from the magnetic moment, which we isolate by combining them in the ratio

$$Z_r \equiv \frac{Z_+(\tilde{\mathcal{E}}) - Z_-(\tilde{\mathcal{E}})}{Z_+(\tilde{\mathcal{E}}) + Z_-(\tilde{\mathcal{E}})} = \frac{\tilde{\mathcal{E}}\tilde{\mu}_B(\tilde{\mathcal{E}})}{2\tilde{m}_B^2}. \tag{14}$$

A simultaneous fit of $\tilde{E}_B$ to Eq. (5) and the amplitude ratio in Eq. (14) allows us to determine both $\tilde{C}_F$ and $\tilde{\mu}_B$. To extract the polarizability $\tilde{C}_F$ we use a fully correlated quadratic fit following Eqs. (4) and (5). Once again we incorporate quadratic terms to both $\tilde{C}_F$ [as in Eq. (11)] and $\tilde{\mu}_B$,

TABLE I.   Results for the polarizabilities and magnetic moments of the baryonic composites of a strongly coupled $SU(N_D)$ theory, in lattice units.

N_D	$m_{\rm PS}/m_V$	$\tilde{m}_B$	$\alpha\tilde{C}_F$	$\alpha^2\tilde{C}'_F$	$\tilde{\mu}_B$	$\tilde{\mu}'_B$	$\chi^2/{\rm d.o.f.}$
4	0.77	0.98204(93)	0.1420(56)	−0.089(29)	$\cdots$	$\cdots$	0.7/3
	0.70	0.88805(113)	0.1514(106)	−0.142(68)	$\cdots$	$\cdots$	4.8/3
3	0.77	0.69812(51)	0.2829(127)	−0.177(45)	−6.87(26)	714(103)	3.0/7
	0.70	0.61904(59)	0.2829(81)	−0.165(24)	−5.55(18)	396(78)	13.4/7

$$\tilde{\mu}_B(\tilde{\mathcal{E}}) = \tilde{\mu}_B + \tilde{\mu}'_B|\tilde{\mathcal{E}}|^2. \qquad (15)$$

The polarizability results for both SU(4) and SU(3) are presented in Table I, and results for the energies and the ratio Z_r vs background field for the $m_{\rm PS}/m_V = 0.70$ ensembles are plotted in Fig. 1.

Constructing the dimensionless product $\alpha\tilde{C}_F\tilde{m}_B^3$ (as needed for the DM cross section), we find that the SU(4) polarizabilities are larger than SU(3) by about 50%. Thus, we find the SU(3) and SU(4) polarizabilities to be comparable when normalized to the baryon mass. Of course, the baryon mass itself scales proportional to N_D; if we were to set the scale using a quantity such as the string
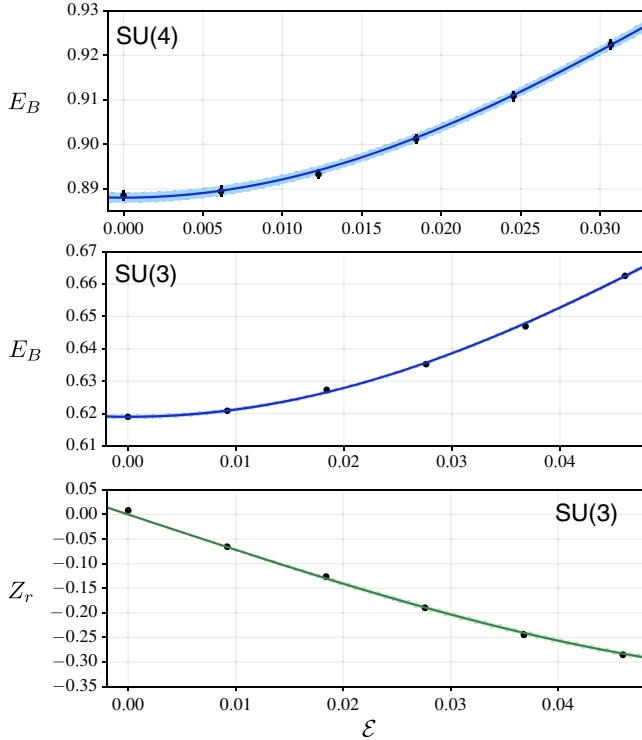

FIG. 1 (color online).   The ground state energy (in lattice units) vs applied electric field $\mathcal{E}$ for SU(4) baryons (top) and SU(3) baryons (middle), and ratio of projected SU(3) correlators vs $\mathcal{E}$ (bottom). Their relations to the magnetic moment and polarizabilities are presented in Eqs. (4), (5), and (14). Results shown are for the ensembles with $m_{\rm PS}/m_V = 0.70$.

tension which does not scale with N_D, then the SU(3) polarizability would be larger.

The effect of the quenched approximation, in which dynamical fermion loops are omitted from the lattice calculation, is not straightforward to estimate. However, the effects of such loops are expected to be suppressed with large N_D and heavy fermion mass; we note that even for QCD with its much lighter fermions, the effects of quenching are generally at most of order 10% [42].

Our calculations are performed at a single lattice spacing and volume, both of which can lead to additional systematic effects. We expect all of these corrections to be small relative to the order of magnitude uncertainty taken for the nuclear matrix element M_F^A. As a cross-check, we note that the neutron polarizability from the Particle Data Group review [43] gives $C_F m_n^3 \simeq 0.36$ at the QCD physical ratio $m_{\rm PS}/m_V = 0.18$, while our SU(3) lattice simulations give $C_F m_B^3 \simeq 0.84$ at $m_{\rm PS}/m_V = 0.70$. These results are broadly consistent with the expected scaling of the polarizability and baryon mass with $m_{\rm PS}$.

Direct detection cross sections.—To relate the dimensionless lattice results to the dimensionful DM mass, m_B, that we vary continuously in order to scan the parameter space of the theory, it is most convenient to give units to the lattice spacing $a = \tilde{m}_B/m_B$. Along with Eq. (8), this leads to the physical value of the polarizability

$$C_F = 4\pi\alpha\left(\frac{\tilde{m}_B}{m_B}\right)^3\tilde{C}_F. \qquad (16)$$

Putting everything together, the spin-independent cross section written as the conventional *per nucleon* rate for a nucleus with (Z, A) from Eq. (2) becomes

$$\sigma_{\rm nucleon}(Z, A) = \frac{Z^4}{A^2}\frac{144\pi\alpha^2\mu_{nB}^2(M_F^A)^2}{m_B^6 R^2}[\alpha\tilde{m}_B^3\tilde{C}_F]^2, \qquad (17)$$

where we use our lattice results in Table I to evaluate the factor in square brackets. We emphasize that, unlike Higgs exchange, the cross section *per nucleus* scales as Z^4 and not A^2, and so the cross section *per nucleon* must be calculated for each nucleus separately in order to compare with experiment. The strongest bound on the spin-independent direct detection scattering rate is from LUX [1]. In Fig. 2, we show the scattering cross section per nucleon for xenon,
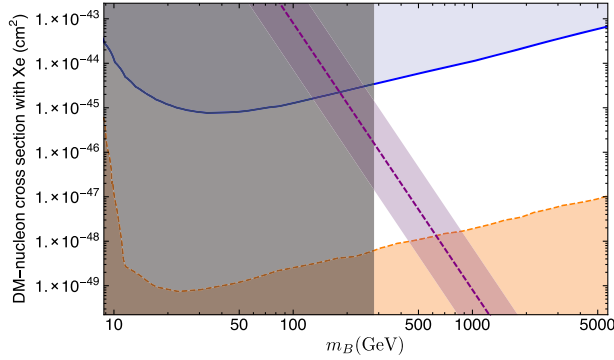
FIG. 2 (color online). The DM spin-independent scattering cross section per nucleon evaluated for xenon is shown as the purple band obtained from the SU(4) polarizability, where the width of the band corresponds to $1/3 < M_F^A < 3$ from low to high. The blue curve and the light blue region above it are excluded by the LUX constraints [1]. The vertical, darker shaded region is excluded by the LEP II bound on charged mesons [23]. The orange region represents the limit at which direct detection experiments will be unable to discriminate DM events from coherent neutrino recoil [44]. We emphasize that this plot is applicable for xenon, and would require calculating Eq. (17) to apply to other nuclei.

and compare with the LUX bounds. We plot only the $N_D = 4$ case here, as the $N_D = 3$ baryons are already excluded up to ~ 20 TeV in mass by the LUX bounds through their magnetic moments [12].

Discussion.—Our lattice results have allowed us to calculate the spin-independent scattering cross section of SU(4) stealth DM through polarizability, which we compare against the LUX constraints in Fig. 2. In units of the stealth baryon mass, we find that the SU(4) polarizability is somewhat larger than that of an SU(3) baryon by about 50%, strongly disfavoring the possibility that the polarizability might be suppressed for baryons in even-N_D gauge theories. The numerical similarity of SU(3) and SU(4) baryon polarizabilities hints that this quantity may be largely independent of N_D in this fermion mass range to first approximation, which would suggest our direct-detection predictions may well generalize for larger N_D.

We find DM masses less than about 200 GeV are excluded, while the DM mass range 200–700 GeV could be probed by future experiments before reaching the neutrino background [44]. Currently, the strongest lower bound on the DM mass arises indirectly from the constraints on the lighter electrically charged mesons that can be produced and decay promptly in collider experiments. Using our results [23], we estimate that DM masses below about 280 GeV are excluded given the LEP II bounds on the pseudoscalar mesons for $N_D = 4$ and the fermion masses considered here.

It is remarkable that a composite DM particle with a weak-scale mass, composed of dark fermions charged under the weak and electromagnetic interaction, can

nevertheless be safe from both direct detection constraints and the LEP II constraint once $m_B \gtrsim 300$ GeV. This suggests there is a serious opportunity for future direct detection experiments to probe the model. Given that the scattering cross section per nucleon scales as $Z^4/(A^2 R^2)$ in Eq. (17), the experiments with the largest nuclei are often more sensitive; i.e., xenon is 3.4 times more sensitive than argon if both experiments reach the same limit on the (conventional) spin-independent scattering per nucleon through Higgs exchange. Comparison of positive results from several experiments can thus provide a clear way to distinguish stealth dark matter interacting via polarizability from ordinary WIMPs interacting via Higgs boson exchange, which will give cross sections simply scaling as A^2.

With our lattice calculation of the dark matter polarizability in this model, the dominant remaining uncertainty stems from the treatment of the nonperturbative nuclear matrix element in Eq. (2), which is similar to the matrix elements required for double beta decay. A significant source of uncertainty is, for example, the presence of excited states in Xe-129 and Ge-73 that have energies of 30 and 15 keV, which will be probed by the loop in the cross section calculation (typical momenta exchanges are roughly at the MeV scale). These resonances could appreciably change the resulting cross section, though the steep dependence on the dark matter mass suggests only a modest equivalent shift of the DM mass.

The brightest opportunity for stealth dark matter discovery may fall within the domain of the Large Hadron Collider (and future colliders). Meson phenomenology is very promising, since charged mesons can be produced through electroweak processes and decay completely into SM particles. In contrast, production of the stealth baryon is rare, since it is considerably heavier than the mesons and would have form factor suppression. This implies the standard missing energy signals that arise from DM production and escape from the detector are *rare*.

Finally, there are many avenues for further investigation of stealth dark matter, detailed in Ref. [23]. One vital issue is to better estimate the abundance. In the DM mass regime where stealth DM is detectable at direct detection experiments, the abundance of stealth dark matter can arise naturally from an asymmetric production mechanism [23] that was considered long ago [7–9] and more recently reviewed in Ref. [45]. If there is indeed an asymmetric abundance of bosonic dark matter, there are additional astrophysical consequences [46–48] that warrant further investigation to constrain or probe stealth DM.

*Present address: Higgs Centre for Theoretical Physics, School of Physics & Astronomy, The University of Edinburgh, EH9 3FD, United Kingdom.

[1] D. Akerib *et al.* (LUX Collaboration), Phys. Rev. Lett. **112,** 091303 (2014).

[2] R. Agnese *et al.* (SuperCDMS Collaboration), Phys. Rev. Lett. **112,** 241302 (2014).

[3] P. Cushman *et al.*, arXiv:1310.8327.

[4] M. Xiao *et al.* (PandaX Collaboration), Sci. China Phys. Mech. Astron. **57,** 2024 (2014).

[5] S. Nussinov, Phys. Lett. **165B,** 55 (1985).

[6] R. S. Chivukula and T. P. Walker, Nucl. Phys. **B329,** 445 (1990).

[7] S. M. Barr, R. S. Chivukula, and E. Farhi, Phys. Lett. B **241,** 387 (1990).

[8] S. M. Barr, Phys. Rev. D **44,** 3062 (1991).

[9] D. B. Kaplan, Phys. Rev. Lett. **68,** 741 (1992).

[10] R. Lewis, C. Pica, and F. Sannino, Phys. Rev. D **85,** 014504 (2012).

[11] A. Hietanen, C. Pica, F. Sannino, and U. I. Sondergaard, Phys. Rev. D **87,** 034508 (2013).

[12] T. Appelquist, R. C. Brower, M. I. Buchoff, M. Cheng, S. D. Cohen, G. T. Fleming, J. Kiskis, M. F. Lin, E. T. Neil, J. C. Osborn, C. Rebbi, D. Schaich, C. Schroeder, S. N. Syritsyn, G. Voronov, P. Vranas, and J. Wasem (Lattice Strong

[13] A. Hietanen, R. Lewis, C. Pica, and F. Sannino, J. High Energy Phys. 12 (2014) 130.

Dynamics (LSD) Collaboration), Phys. Rev. D **88,** 014502 (2013).

[14] T. Appelquist, E. Berkowitz, R. C. Brower, M. I. Buchoff, G. T. Fleming, J. Kiskis, G. D. Kribs, M. Lin, E. T. Neil, J. C. Osborn, C. Rebbi, E. Rinaldi, D. Schaich, C. Schroeder, S. Syritsyn, G. Voronov, P. Vranas, E. Weinberg, and O. Witzel (Lattice Strong Dynamics (LSD) Collaboration), Phys. Rev. D **89,** 094508 (2014).

[15] W. Detmold, M. McCullough, and A. Pochinsky, Phys. Rev. D **90,** 115013 (2014).

[16] W. Detmold, M. McCullough, and A. Pochinsky, Phys. Rev. D **90,** 114506 (2014).

[17] Z. Fodor *et al.*, *Proc. Sci*, LATTICE2014 (2015) 270.

[18] R. S. Chivukula, A. G. Cohen, M. E. Luke, and M. J. Savage, Phys. Lett. B **298,** 380 (1993).

[19] J. Bagnasco, M. Dine, and S. D. Thomas, Phys. Lett. B **320,** 99 (1994).

[20] M. Pospelov and T. ter Veldhuis, Phys. Lett. B **480,** 181 (2000).

[21] G. D. Kribs, T. S. Roy, J. Terning, and K. M. Zurek, Phys. Rev. D **81,** 095001 (2010).

[22] M. R. Buckley and E. T. Neil, Phys. Rev. D **87,** 043510 (2013).

[23] T. Appelquist, R. C. Brower, M. I. Buchoff, G. T. Fleming, X.-Y. Jin, J. Kiskis, G. D. Kribs, E. T. Neil, J. C. Osborn, C. Rebbi, E. Rinaldi, D. Schaich, C. Schroeder, S. Syritsyn, P. Vranas, E. Weinberg, and O. Witzel (Lattice Strong Dynamics (LSD) Collaboration), Phys. Rev. D **92,** 075030 (2015).

[24] Y. Bai and R. J. Hill, Phys. Rev. D **82,** 111701 (2010).

[25] M. Frigerio, A. Pomarol, F. Riva, and A. Urbano, J. High Energy Phys. 07 (2012) 015.

[26] Y. Hochberg, E. Kuflik, T. Volansky, and J. G. Wacker, Phys. Rev. Lett. **113,** 171301 (2014).

[27] Y. Hochberg, E. Kuflik, H. Murayama, T. Volansky, and J. G. Wacker, Phys. Rev. Lett. **115,** 021301 (2015).

[28] M. E. Luke, A. V. Manohar, and M. J. Savage, Phys. Lett. B **288,** 355 (1992).

[29] A. L. Fitzpatrick, W. Haxton, E. Katz, N. Lubbers, and Y. Xu, arXiv:1211.2818.

[30] A. L. Fitzpatrick, W. Haxton, E. Katz, N. Lubbers, and Y. Xu, J. Cosmol. Astropart. Phys. 02 (2013) 004.

[31] R. J. Hill and M. P. Solon, Phys. Rev. D **91,** 043504 (2015).

[32] R. J. Hill and M. P. Solon, Phys. Rev. D **91,** 043505 (2015).

[33] M. T. Frandsen, U. Haisch, F. Kahlhoefer, P. Mertsch, and K. Schmidt-Hoberg, J. Cosmol. Astropart. Phys. 10 (2012) 033.

[34] N. Weiner and I. Yavin, Phys. Rev. D **86,** 075021 (2012).

[35] G. Ovanesyan and L. Vecchi, J. High Energy Phys. 07 (2015) 128.

[36] J. Kotila and F. Iachello, Phys. Rev. C **85,** 034316 (2012).

[37] M. T. Mustonen and J. Engel, Phys. Rev. C **87,** 064302 (2013).

[38] W. Detmold, B. C. Tiburzi, and A. Walker-Loud, Phys. Rev. D **79,** 094505 (2009).

[39] W. Detmold, B. C. Tiburzi, and A. Walker-Loud, Phys. Rev. D **81,** 054502 (2010).

[40] R. G. Edwards and B. Joo (SciDAC), Nucl. Phys. B, Proc. Suppl. **140,** 832 (2005).

[41] G. S. Bali and F. Bursa, J. High Energy Phys. 09 (2008) 110.

[42] G. Colangelo *et al.*, Eur. Phys. J. C **71**, 1695 (2011).
[43] K. A. Olive *et al.* (Particle Data Group), Chin. Phys. C **38**, 090001 (2014).
[44] J. Billard, E. Figueroa-Feliciano, and L. Strigari, Phys. Rev. D **89**, 023524 (2014).
[45] K. M. Zurek, Phys. Rep. **537**, 91 (2014).
[46] S. D. McDermott, H.-B. Yu, and K. M. Zurek, Phys. Rev. D **85**, 023519 (2012).
[47] J. Bramante, K. Fukushima, and J. Kumar, Phys. Rev. D **87**, 055012 (2013).
[48] B. Bertoni, A. E. Nelson, and S. Reddy, Phys. Rev. D **88**, 123505 (2013).